# Physical disruption of gel particles on the macroscale does not affect the study of protein gel structure on the micro or nanoscale

Meltem Bayrak, Jitendra P Mata, Andrew E Whitten, Charlotte E Conn, Juliane Floury, Amy Logan

Colloid and Interface Science Communications 46 (2022) 100574

Contents lists available at ScienceDirect

Colloid and Interface Science Communications

journal homepage: www.elsevier.com/locate/colcom

Rapid Communication

# Physical disruption of gel particles on the macroscale does not affect the study of protein gel structure on the micro or nanoscale

Meltem Bayrak [a,c], Jitendra P. Mata [b,*], Andrew E. Whitten [b], Charlotte E. Conn [c], Juliane Floury [d], Amy Logan [a,*]

[a] CSIRO Agriculture and Food, 671 Sneydes Road, Werribee, Victoria 3030, Australia
[b] Australian Centre for Neutron Scattering, Australian Nuclear Science and Technology Organisation, Lucas Heights, NSW 2234, Australia
[c] School of Science, College of Science, Engineering and Health, RMIT University, 124 LaTrobe Street, Melbourne, VIC 3000, Australia
[d] STLO, INRAE, Institut Agro, 35042 Rennes, France

ARTICLE INFO

*Keywords:*
Casein gel
Structure
Neutron scattering
Physical disruption
Blending

ABSTRACT

Small and Ultra Small Angle Neutron Scattering (SANS and USANS) are commonly used techniques for the nano- and microstructural characterisation of systems such as polymers, gels, and aggregates. In many cases, for practical purposes, disruption of the larger structures into smaller particles may be necessary to meet the requirements of the specific sample environment used. However, a lack of knowledge about its effect on the nano- and microstructure prevents the adoption of this simple approach. In our study, we used a newly developed recirculated flow set-up designed for the *in-situ* measurement of blended transglutaminase-induced acid gels (TG). The average gel size reduction of distributions examined herein ($d_{50}$; 1020, 462, and 294 μm) did not noticeably alter the integrity of gel structure at the interior of the particle. This study validates the proposed approach as an effective way to examine structural elements at a micro- or nanoscale using *in-situ* neutron scattering techniques.

## 1. Introduction

The structural characterisation of gel systems *via* small-angle X-ray or neutron scattering is a well-established technique. A Scopus search (October 2021) retrieved nearly 5000 papers using the keywords "small-angle scattering" and "gel". Among the various techniques available for structural characterisation, neutron scattering is a particularly powerful tool, and the structural characterisation of gel systems has been conducted using small-angle scattering since the 1940s [1]. While it is advantageous to measure samples in their natural state, various sample environments used with small-angle scattering may require the study of mechanically deformed structures to produce smaller or thinner particles [2–5]. The main advantage of the physical blending of particles is to produce homogenous samples and could benefit several disciplines. For instance, nanoscopic air bubbles trapped on hydrophobic surfaces, especially in $D_2O$ (deuterium oxide), that cause background noise due to scattering from the air [2] could be eliminated by disrupting those bubbles by mechanical disruption. The small-angle scattering spectra in samples with high content of hydrogenous material is dependent on the sample thickness. These samples may suffer 'multiple scattering' which has a significant effect on data analysis. High-density samples could be processed into smaller or thinner pieces to remove the effects of multiple scattering while providing better coverage in a sample cell. In most small-angle scattering studies of high-density rocks or minerals, samples are usually prepared at varying thicknesses to verify multiple scattering has not led to any unwanted complication [3–5]. However, there is usually an experimental limit on how thin a sample can be made and thus grinding the samples into smaller pieces may be a straightforward approach if no effect on the micro- and nanostructure is ensured. Furthermore, examination of gels under flow may require their physical disruption into smaller sized particles to facilitate the flow of polymers, gels, aggregates, and minerals at a macroscale. While sample environments such as flow cells and tumblers are available for time-resolved small-angle neutron scattering experiments [6], their application is limited to materials with a maximum diameter of 1 mm due to the path length of a sample cell. The simultaneous characterisation of a blended soft matter structure using a time-resolved neutron scattering experiment will benefit several studies such as dynamics in swelling of

* Corresponding authors.
*E-mail addresses:* jtm@ansto.gov.au (J.P. Mata), amy.logan@csiro.au (A. Logan).

https://doi.org/10.1016/j.colcom.2021.100574
Received 8 October 2021; Received in revised form 30 November 2021; Accepted 14 December 2021
Available online 27 December 2021

hydrogels, characterisation of particles in motion or changes in structure when exposed to different environmental conditions. Flow-through time-resolved small-angle X-ray scattering has been specifically used to investigate the digestion of colloidal systems in solution [7–9]. Real-time structural analysis of solid particles is critical for developing a fundamental understanding of bioactive compound delivery systems in personalised food structures during digestion. While physical grinding or blending may appear to be a simple solution to the problem a lack of knowledge about its effects on nano and microstructure prevents greater uptake of this simple approach.

This study examines the effect of physical blending on the micro- and nanostructure of a transglutaminase-induced acid gel (TG), model system, prepared from micellar casein. Acidification decreases the negatively charged groups at the casein micelle surface resulting in micellar aggregation, followed by the cross-linking of proteins between glutamine and lysine residues using the enzyme transglutaminase [10,11]. Transglutaminase is commonly used in the industry to modify protein functionality [12,13]. For example, it is often used to manufacture yoghurts with a firmer consistency and with less syneresis compared to a standard acid gel [10,14–17]. Several neutron scattering studies have investigated the structure of similar hydrogels as well as oleogels, and polymer gels [18–22]. The structure of TG in $H_2O$ (water) has been previously studied by the authors using scattering techniques, in combination with rheology, and scanning and transmission electron microscopy [23]. TG was found to be composed of fine filamentous protein strands with a homogeneous microstructure formed by the cross-linking of numerous neighboring micelles aggregate at junction points throughout the gel network. It has previously been demonstrated that TG is predominantly degraded during mixing due to surface erosion [23]. TG is more difficult to disrupt due to these stronger and more numerous interactions, and therefore an ideal model system to use in the current study for the systematic and time-resolved analysis of gel particle structure as a function of blending time, hence degree of disruption.

In this study, we investigated an approach to practically prepare homogenous gel samples by blending, as a method of physical disruption at a macroscale, and demonstrated whether there would be an effect on the micro- and nanostructure of TG. Gels of varying particle size distribution were produced in simulated gastric fluid by hand blending for an increasing length of time; USANS and SANS analysis was subsequently used to characterise the structure of the deformed gels of three different particle size distributions by fitting the scattering pattern to simple models. This study will assist future experimentalists in preparing their sample with ease, knowing that the structure at the interior of the smaller gel particles does not significantly change between the 1 nm and 20 μm length scale.

## 2. Materials and methods

### 2.1. Materials

Micellar casein powder (PRODIET 85B, 82.41% protein) was purchased from Ingredia (Arras, France). Transglutaminase (ACTIVA WM; 100 U $g^{-1}$) was kindly provided by Ajinomoto Foods Europe, Japan. Sodium azide (S2002), D-(+)-Gluconic acid δ-lactone (G4750), KCl (P3911), $KH_2PO_4$ (P0662), $NaHCO_3$ (S6014), NaCl (S9888), $MgCl_2$ (M8266), $(NH_4)_2CO_3$ (207861), HCl (320331), and $CaCl_2$ (C1016) were purchased from Sigma-Aldrich, Inc. (St. Louis, MO, USA).

### 2.2. Preparation of casein gels and their deformation by blending

Micellar casein powder (10%, *w/v*) solutions in $H_2O$ (water) were prepared according to Bayrak et al. [23] to achieve solubilisation of >98%. In brief, sodium azide (0.02%, *w*/w) was added to the solution to prevent microbial growth. The solution was homogenised using an Ultra-Turrax homogeniser (IKA, Germany) at 10,000 rpm for 5 min, followed by stirring (150 rpm; 2mag MIXdrive 15HT, 2mag AG, Munich, Germany) at 50 °C for 6 h after which the homogenisation step was repeated. Stirring continued overnight at room temperature. In order to prepare the TG (10% *w*/w), the micellar casein powder solution was warmed to 40 °C for 1 h in a water bath, followed by the addition of 1.1% (*w*/w) glucono δ-lactone and transglutaminase powder with a final concentration of 5 U $g^{-1}$ with stirring at 700 rpm for 30 s. The solution was allowed to gelatinise in a water bath at 40 °C for 1 h [23].

Simulated gastric fluid (pH 6.5, 60 mL), without pepsin enzyme, was prepared as described by Brodkorb et al. [24] and combined with TG (40 g) to replicate the environmental conditions under which gastric digestion would take place. The gastric fluid, which contains a low concentration of salts that act as a buffer, does not contain any digestive enzyme. This allows for the real-time measurement of protein structure within the *in situ* flow setup using an experimentally appropriate buffer. The ratio of simulated gastric fluid to gel (3:2) used herein was selected to ensure optimal neutron scattering intensity (data not shown). Then, gel samples were broken into fragments of varying particle size range using a hand blender (Braun Miniprimer 3, Germany) for 10 s (MT10), 20 s (MT20) and 30 s (MT30). A portion of gel was retained without blending in simulated gastric fluid as the Control gel. In contrast to the blended samples, which were suspended in simulated gastric fluid and circulated through the sample cell, the Control gel was packed into the sample cell window without excess fluid and held static. To allow a direct comparison, the Control scattering intensity was shifted in the y-axis direction to account for the 3:2 dilution of TG in simulated gastric fluid experienced by blended samples. The gels were prepared on two different occasions for the scattering studies, gel particle size analysis and viscosity measurements.

### 2.3. Characterisation of gel fragments

The median ($d_{50}$ - half the particles in solution are smaller and half larger than this diameter), $d_{10}$ (10% of particles in solution are smaller than this diameter) and $d_{90}$ (90% of particles in solution are smaller than this diameter) particle size distribution of the MT10, MT20 and MT30 gel fragments were measured by particle size analysis (Mastersizer3000, Malvern Instruments, England) using a refractive index of 1.462 and 1.33 for the casein and $H_2O$, respectively [23]. Duplicate measurements were performed for independently prepared samples.

The viscosity measurements of the gel particles in simulated gastric fluid were carried out according to Laiho et al. [25] using an Anton Paar-Physica rheometer (MCR 302, Anton Paar Physica, Physica Meßtechnik GmbH, Stuttgart, Germany) with a cup and 6-blade vane geometry. The viscosity was measured over an increasing shear rate of 0.01–1000 $s^{-1}$. For each sample, the viscosity (Pa•s) measurement was performed in independently prepared triplicate samples.

### 2.4. Investigation of the gel structure with ultra-small (USANS) and small-angle (SANS) neutron scattering

The USANS and SANS measurements were performed at the Australian Nuclear Science and Technology Organisation on the KOOKABURRA (USANS) and BILBY (SANS) instruments, respectively [26,27]. The USANS measurements were performed to cover a $q$-range of $3.5 \times 10^{-5}$ $Å^{-1}$ to 0.008 $Å^{-1}$. USANS data were collected using long wavelength of 4.74 $Å^{-1}$. Data were reduced using in-house developed python script in GumTree software. Empty cell scattering data were subtracted from the sample and data were then converted to absolute scale and then desmeared. The SANS collection was performed in time-of-flight mode with a wavelength range of $\lambda = 2$–20 Å, and a wavelength resolution of $\Delta\lambda/\lambda = 0.12$. With an array of detectors positioned at 7.000 m, 3.000 m and 2.000 m, a $q$-range of 0.00224–0.55481 $Å^{-1}$ was covered in a single measurement. The collimation length used was 6.800 m and source and sample apertures were both circular with diameters of 40 mm and 12.5 mm, respectively. Reduction of the SANS data was carried out using Mantid, data analysis and visualisation

package [28], correcting for sample transmission, background radiation, sample thickness and solvent scattering. Data were placed on an absolute scale using the transmission of the empty beam. The reduced USANS and SANS data were then combined to give full $q$-range scattering curves. Each gel sample was prepared separately for USANS and SANS measurements and the scattering pattern of samples were determined in duplicate. The sample cell with a path length of 1 mm was used in both the USANS and SANS measurements. Neutron scattering modelling was analysed using SasView software (http://sasview.org). The flow setup validated in this experiment (Fig. 1) was designed for a large-scale *in situ* experiment, using physically disrupted casein gels, and will be demonstrated further in our future research. In brief, blended gel particles in digestive fluid were circulated through the sample cell (1 mm path length) at a 10 mL $min^{-1}$ rate.

### 2.5. Statistical analysis

Data was analysed for statistical differences between samples by one-way analysis of variance (ANOVA) using RStudio v3 software (RStudio™, Boston,MA, USA) with "Tukey HSD" function. To measure differences in mean values, a $p$ value $<0.05$ was considered to be statistically significant.

## 3. Results and discussion

### 3.1. Characterisation of gel particle size on the macroscale

The aim of this study was to examine the hypothesis that a reduction in gel particle size (within the limits examined herein) would not alter the integrity of the localised protein network on the micro- or nano-length scale, as measured using USANS and SANS. To achieve this, TG and simulated gastric fluid mixtures were exposed to one of the three blending conditions to create samples of different particle size distribution (Fig. 2). The distributions of TG particles were within the 5–6 μm to ~3.5 mm size range. The median gel particle size ($d_{50}$) decreased with blending time from 1027.0 ± 96.2 μm (10 s blending) to 293.8 ± 2.9 μm (30 s blending) (Table 1), with a minimum particle size of around 5–6 μm in all three preparations (Fig. 2). After 10 s of blending, just under half of the particles remained bigger than 1 mm in diameter (Fig. 2-insert). An increase in blending time to 20 s resulted in a significant ($p < 0.05$) shift in the distribution peak; this blending method resulted in less than 10% of gel particles remaining above 1 mm in diameter. Blending for 30 s reduced the particles' size further, where less than 1% of gel particles were above 1 mm in size. The relative sizes of the casein gel fragments are represented in Fig. 4.

The apparent viscosity as a function of shear rate and shear stress was

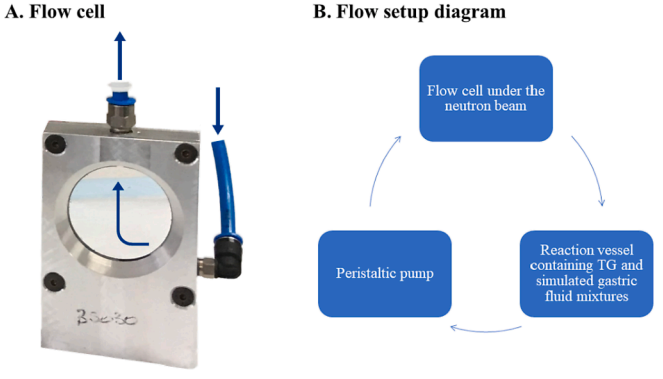


**Fig. 1.** Sample flow cell with an inlet on the side and outlet on top, with the arrows showing the direction of flow. The window diameter is 40 mm and the width of sample cell for gel particles to flow through is 1 mm. The flow rate was 10 mL $min^{-1}$ (A). A diagram showing the process of circulation of gel particles (B).

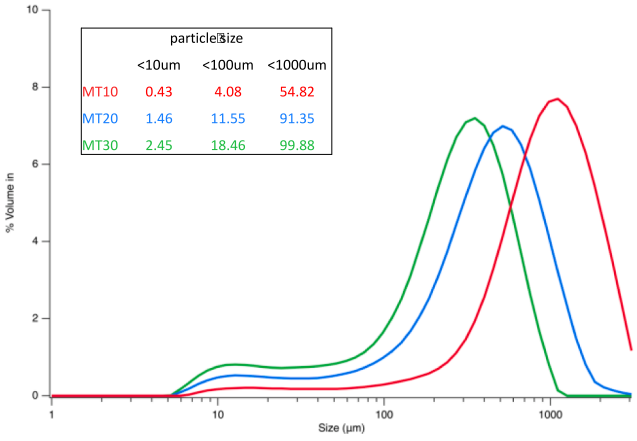


**Fig. 2.** The particle size distribution of 10% (*w/v*) Transglutaminase induced acid gel (TG) samples that were blended for 10 s (MT10 - red), 20 s (MT20 - blue) and 30 s (MT30 – green). (For interpretation of the references to colour in this figure legend, the reader is referred to the web version of this article.)

**Table 1**
The diameter of gel particles where 10% ($d_{10}$), 50% ($d_{50}$) and 90% ($d_{90}$) (mean ± S.D., $n = 4$) of 10% (*w/v*) Transglutaminase induced acid gel (TG) particles are smaller for each processing condition. All values are the mean of duplicate preparation ± the standard deviation. Values marked with different letters in the same column are significantly different across samples ($P < 0.05$).

| Sample | $d_{10}$ (μm) | $d_{50}$ (μm) | $d_{90}$ (μm) |
|---|---|---|---|
| MT10 | $340.0 \pm 44.9^{a}$ | $1027.0 \pm 96.2^{a}$ | $2167.5 \pm 125.0^{a}$ |
| MT20 | $90.5 \pm 8.2^{b}$ | $469.0 \pm 70.8^{b}$ | $1058.0 \pm 181.2^{b}$ |
| MT30 | $40.6 \pm 6.0^{c}$ | $293.8 \pm 2.9^{c}$ | $647.5 \pm 10.8^{c}$ |

measured for all three samples to confirm that particle size did not influence the flow properties of the circulated samples during an *in situ* small-angle scattering experiment (Fig. 3). As expected, the flow viscosity measurements confirmed that the significant difference in blended gel particle sizes did not affect the system flow properties and hence this variable can be considered to have no effect on the integrity of results. For all samples, the apparent shear viscosity values decreased at the same rate with increasing shear rate, indicating the solid-like behaviour of the material at rest.

### 3.2. Characterisation of gel structure on the nano and microscale

USANS measurements were obtained over a $q$-range from $3.5 \times 10^{-5}$

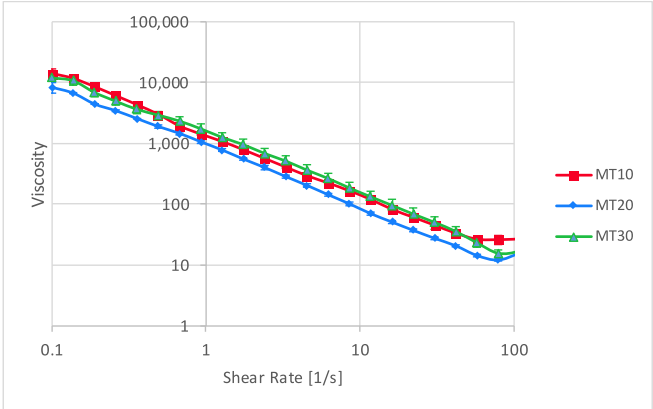


**Fig. 3.** The average viscosity (Pa*s) as a function of shear rate (1 $s^{-1}$) ± standard deviation of TG in the gastric fluid for different gel particle size distributions of MT10, MT20 and MT30.

$Å^{-1}$ to 0.008 $Å^{-1}$, corresponding to spacings in the range 18 μm to 79 nm. No gel particles were noted below 5–6 μm (Fig. 2). The SANS measurements were made with a $q$-range of 0.00224 to 0.55481 $Å^{-1}$, which corresponds to a size scale of approximately 280 nm to 1.13 nm. This length scale is smaller than any gel particle studied here, thus the SANS measurements are sensitive to the internal structure of the gel particles (casein micelle in Fig. 4). Fig. 5 shows the combined scattering curves obtained by USANS (low-$q$) and SANS (mid- to high-$q$). It is important to note that the combined SANS and USANS measurements are obtained from separate experiments and hence different samples. Gel samples for USANS and SANS measurements were prepared and mixed with the simulated gastric fluid separately. Overlap of the resulting scattering curves provides good evidence for the repeatability of the blending and scattering experimental conditions within samples. The dashed vertical lines in Fig. 5 represent the area at which the USANS and SANS curves overlap. The scattering intensity of the Control was higher than the blended samples (Fig. A1). This is because the sample holder in the beam would have contained more Control gel by volume than blended gels at any given time, with the gel particles for MT10, MT20 and MT30 dispersed in simulated gastric fluid and circulated through the sample holder. Thus, $I(q)$ for the Control scattering pattern was scaled by a constant, correcting for the amount of sample under the neutron beam. The likelihood that recirculation over an extended period of time may lead to the progressive disruption of gel particles was tested by observing the scattering patterns of a gel circulated within the *in-situ* flow set-up for 1 h. No change in scattering pattern was observed between the first 10 min compared to the last 10 min (data not shown), indicating that we can be confident that observed effects are the result of experimental factors (such as changes in structure over the course of gastric enzyme digestion) rather than shear effects introduced through the set-up protocol.

The scattering data were fitted with a power law, Guinier-Porod and Gaussian peak models in the low- and mid-$q$ regions, respectively, according to the method described in Bayrak et al. [23] (Fig. 5). The model fit values for the power law exponent, radius of gyration (Å) and dimension variable are shown in Table 2. The power law exponent measured at the ultra-low $q$ region ($q$ ($Å^{-1}$) $<$ 0.0001; $d >$ 6.28 μm) relates to the compactness and density of the protein strand packing of gel microstructure [23,29]. As such, a change in the power law value indicates a difference in the packing and density of the aggregate network structure on a microscale. There was no significant difference ($p < 0.05$) in power law between the Control, MT10, MT20 and MT30 samples. This indicates that the integrity of the gel network structure at the interior of the newly formed particles, with reduced particle size down to 5–6 μm after blending, remained intact. The breaking down or loosening of the gel aggregate microstructure did not occur greatly.

For the mid-$q$ region between 0.0003 and 0.015 $Å^{-1}$ (2.04 μm - 41.3 nm), an estimate of the size and dimensionality of casein aggregates was obtained using the Guinier-Porod model fitting [30]. The radius of gyration represents the size and compactness of casein micelle aggregates within the gel structure [23,31]. A small decrease in the size of the casein aggregates was observed for samples MT20 and MT30, with the radius of gyration decreasing from ~310 to ~300 Å, which indicates a slightly increased shrinking of micelles contained within the aggregate particle of MT20 and MT30, possibly due to the higher surface area provided by the smaller particles, increasing their respective response to the surrounding simulated gastric fluid environment [32] (Table 2). The dimension variable was used to determine whether the objects were shaped like spheres, rods, platelets or other shapes in-between [30]. The results show that the shape of the casein aggregates contained within the protein strands remained unchanged across samples, with a dimension variable value of 1.69 indicating a shape between rod and plate-like structures. With the assumption of having an elongated ellipsoid-like structure that resembles a rod, dimensions for the micelle aggregates are calculated by dividing the square of the length (twice the radius of gyration value in nm) by 12, where a Rg of 300 Å (30 nm) equates to a 300 nm sized object ($60^2/12$). The radius of gyration and dimension variable values remained more or less the same for gels across the different size distributions, suggesting nearly no difference in the shape and size of casein micelles in response to the mechanical deformation (Table 2). The inflection point in the high $q$ region, which corresponds to the CCP (colloidal calcium phosphate) nanoclusters located within the casein micelle structure, has remained unchanged between the Control and blended samples, indicating that no change in internal structure has occurred.

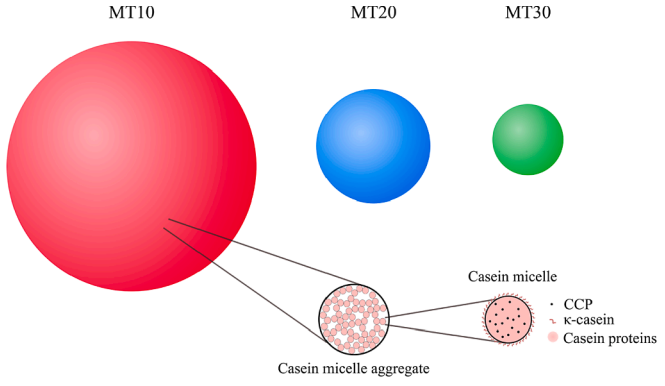


**Fig. 4.** A representation of the relative size of gel particles upon blending; 10 s (MT10), 20 s (MT20) and 30 s (MT30). The gels were made through casein micelle aggregation.

## 4. Conclusion

Herein, we reported the analysis of mechanically disrupted gel particles, where the micro- and nanoscale structural elements within the gel particle are of interest. The wide q-range covered by a combination of USANS and SANS allows to study structural differences potentially induced by mechanical disruption of the gel particles over the size range from 18 μm to 1.13 nm. Despite the fact that the particle size distribution of the blended gels significantly decreased with blending time, their structural characteristics from small angle scattering techniques remained relatively unaffected and were comparable to the Control sample. The data from particle size measurements and neutron scattering has, therefore, demonstrated that the physical disruption of particles for size reduction can be applied as a valid tool for the *in situ* studies of intact samples.

This work has shown that mechanical disruption to form TG particle distributions within the 5–6 μm to ~3.5 mm size range will not influence structural elements at a micro- or nanoscale within the interior of the gel particle. In connection with our results, it has been demonstrated that physical disruption could be used as a method to reduce the sample particle size, removing air bubbles, facilitating sample preparation (*e.g.*, gel loading) or utilising specific sample environments, such as the flow setup examined herein. However, the level of deformation achieved through mechanical disruption will depend on the type and number of chemical bonds for other gel types. TG is one of the most common food gels and was chosen as a model system here, however, our findings are not limited to food gels. The cross-linking of casein proteins by transglutaminase enzyme increases the gel strength of the acid gels examined in the current work, and thus it is important to characterise the microstructures of other systems with different gelation mechanisms and physicochemical properties. This is because large deformation behaviour and gel breakdown will differ for samples of varying strength, harder or weaker. As a result, blending for weaker gels should be done for a shorter period of time to obtain gel particles within the size range investigated here. For some formulations such as weak acid gels, diluting and stirring may be enough to get the gel to flow inside the system. The ionic strength and acidity of the environment should also be

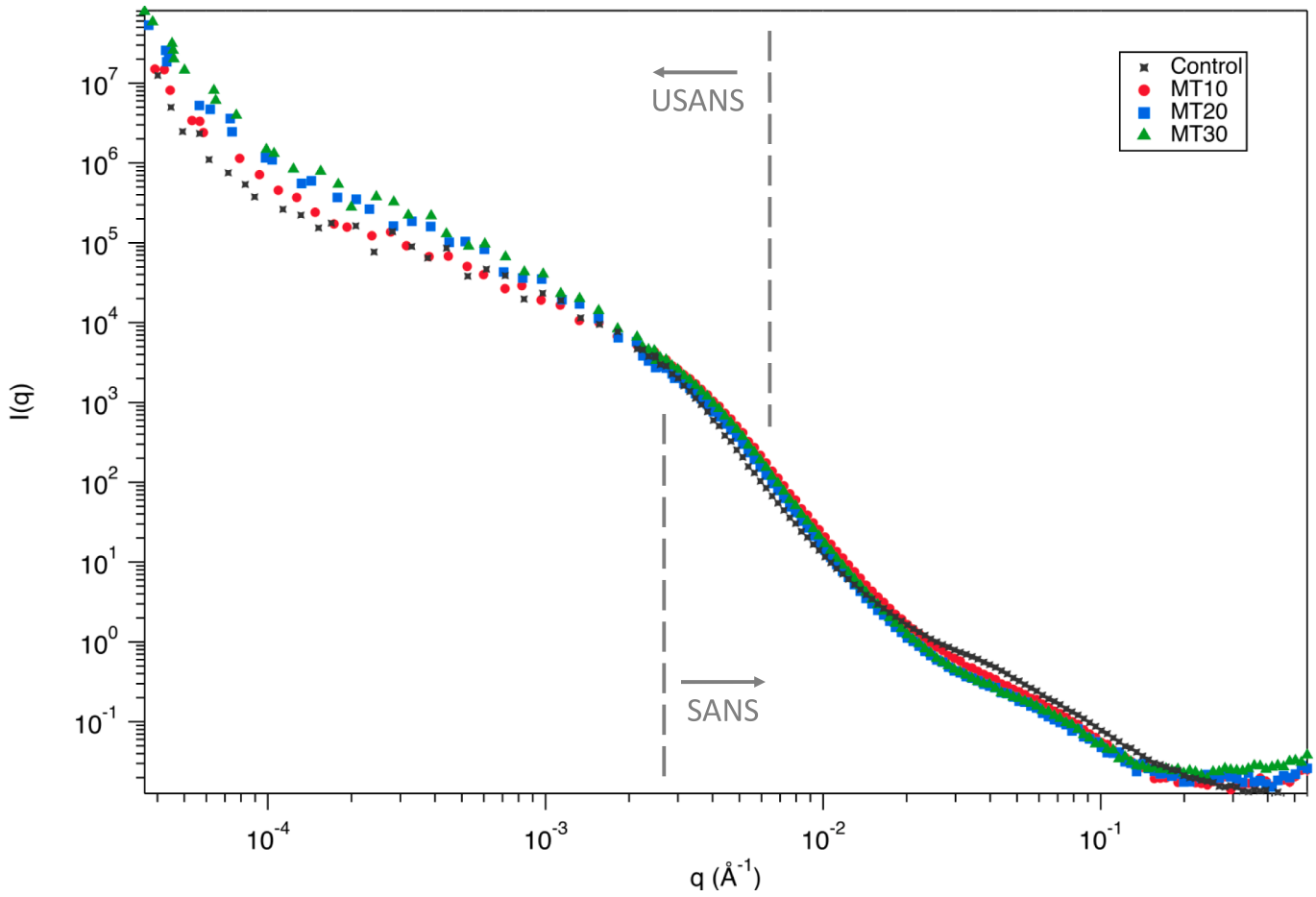


**Fig. 5.** The full q-range of USANS and SANS scattering curve of 10% (*w/v*) Transglutaminase induced acid gel (TG) samples; blended for 10 s (MT10), 20 s(MT20), 30 s (MT30) and the Control. For a clear representation of scattering patterns, the Control scattering pattern was scaled for comparison (see Fig. A1 for the unscaled Control pattern). Each gel sample was prepared separately for USANS and SANS measurements and later combined, indicated by dashed vertical lines (See also Table 2).

**Table 2**
The power law exponent determined by power law fit; and the dimension variable (s) and estimated size of casein aggregates fused together to form network strands calculated as the radius of gyration for 10% (*w/v*) Transglutaminase induced acid gel (TG) samples; blended for 10 s (MT10), 20 s (MT20) and 30 s (MT30) and the Control. All values are the mean of duplicate analyses ± the standard deviation. Values marked with different letters in the same column are significantly different across samples ($P < 0.05$).

| Sample | Power law exponent (q < 0.0001) | Radius of gyration (Å) (0.001 < q < 0.01) | Dimension variable (0.001 < q < 0.01) |
|---|---|---|---|
| Gel (Control) | 3.85 ± 0.00[a] | 310.98 ± 0.00[a] | 1.70 ± 0.01[a] |
| MT10 | 3.85 ± 0.00[a] | 308.01 ± 2.39[a] | 1.70 ± 0.03[a] |
| MT20 | 3.85 ± 0.00[a] | 299.00 ± 2.17[b] | 1.69 ± 0.01[a] |
| MT30 | 3.85 ± 0.00[a] | 300.10 ± 2.06[b] | 1.70 ± 0.01[a] |

addressed for each sample. For instance, due to diffusion and permeability to surrounding fluid relating to the surface area of a gel particle, smaller rennet gel particles (larger surface area) would be predicted to contract more in a low-pH environment than an unblended gel.

Supplementary data to this article can be found online at https://doi.org/10.1016/j.colcom.2021.100574.

## Declaration of Competing Interest

The authors declare that they have no known competing financial interests or personal relationships that could have appeared to influence the work reported in this paper.

The authors declare the following financial interests/personal relationships which may be considered as potential competing interests.

## Acknowledgments

We acknowledge the support of the Australian Nuclear Science and Technology Organisation (ANSTO) in providing USANS and SANS beam facilities (proposal 9587) used in this work. The authors would like to thank AINSE Limited for providing financial assistance (Award - PGRA) to enable work on the BILBY and KOOKABURRA beamlines. We would also like to thank Liliana de Campo (ANSTO) for their assistance with the USANS measurements performed on the KOOKABURRA instrument and Norman Booth (ANSTO) for their assistance with the flow setup. The authors would like to acknowledge the CSIRO AIM Future Science Platform for supporting this work.

## References


[1] C. Shull, L. Roess, X-ray scattering at small angles by finely-divided solids. I. General approximate theory and applications, J. Appl. Phys. 18 (3) (1947) 295–307.
[2] Y.B. Melnichenko, et al., Cavitation on deterministically nanostructured surfaces in contact with an aqueous phase: a small-angle neutron scattering study, Langmuir 30 (33) (2014) 9985–9990.
[3] J. Connolly, et al., Comparison of the structure on the nanoscale of natural oil-bearing and synthetic rock, J. Pet. Sci. Eng. 53 (3–4) (2006) 171–178.
[4] A. Radliński, et al., Fractal geometry of rocks, Phys. Rev. Lett. 82 (15) (1999) 3078.
[5] A.P. Radlinski, Small-angle neutron scattering and the microstructure of rocks, Rev. Mineral. Geochem. 63 (1) (2006) 363–397.
[6] V.S. Urban, et al., Soft matter sample environments for time-resolved small angle neutron scattering experiments: a review, Appl. Sci. 11 (12) (2021) 5566.
[7] S. Salentinig, H. Amenitsch, A. Yaghmur, In situ monitoring of nanostructure formation during the digestion of mayonnaise, ACS Omega 2 (4) (2017) 1441–1446.
[8] C. Hempt, et al., Nanostructure generation during milk digestion in presence of a cell culture model simulating the small intestine, J. Colloid Interface Sci. 574 (2020) 430–440.
[9] A.C. Pham, A.J. Clulow, B.J. Boyd, Formation of self-assembled Mesophases during lipid digestion, Front. Cell Develop. Biol. 9 (2021).
[10] C. Schorsch, H. Carrie, I. Norton, Cross-linking casein micelles by a microbial transglutaminase: influence of cross-links in acid-induced gelation, Int. Dairy J. 10 (8) (2000) 529–539.
[11] M. Hannß, et al., Acid-induced gelation of enzymatically and nonenzymatically cross-linked caseins—texture properties, and microstructural insights, J. Agric. Food Chem. 68 (47) (2020) 13970–13981.
[12] S. Lauber, T. Henle, H. Klostermeyer, Relationship between the crosslinking of caseins by transglutaminase and the gel strength of yoghurt, Eur. Food Res. Technol. 210 (5) (2000) 305–309.
[13] T. Şanlı, et al., Effect of using transglutaminase on physical, chemical and sensory properties of set-type yoghurt, Food Hydrocoll. 25 (6) (2011) 1477–1481.
[14] C. Kuraishi, K. Yamazaki, Y. Susa, Transglutaminase: its utilization in the food industry, Food Rev. Int. 17 (2) (2001) 221–246.
[15] B. Ozer, et al., Incorporation of microbial transglutaminase into non-fat yogurt production, Int. Dairy J. 17 (3) (2007) 199–207.
[16] E. Romeih, G. Walker, Recent advances on microbial transglutaminase and dairy application, Trends Food Sci. Technol. 62 (2017) 133–140.
[17] L. Duarte, et al., Review transglutaminases: part II—industrial applications in food, biotechnology, textiles and leather products, World J. Microbiol. Biotechnol. 36 (1) (2020) 1–20.
[18] M. Shibayama, Small angle neutron scattering on gels, Soft Matt. Character. (2008) 783.
[19] E.P. Gilbert, Small-angle X-ray and neutron scattering in food colloids, Curr. Opin. Colloid Interface Sci. 42 (2019) 55–72.
[20] M. Shibayama, Small-angle neutron scattering on polymer gels: phase behavior, inhomogeneities and deformation mechanisms, Polym. J. 43 (1) (2011) 18–34.
[21] I. Hoffmann, Neutrons for the study of dynamics in soft matter systems, Colloid Polym. Sci. 292 (9) (2014) 2053–2069.
[22] P.W. Schmidt, Small-angle scattering studies of disordered, porous and fractal systems, J. Appl. Crystallogr. 24 (5) (1991) 414–435.
[23] M. Bayrak, et al., Investigating casein gel structure during gastric digestion using ultra-small and small-angle neutron scattering, J. Colloid Interface Sci. 594 (2021) 561–574.
[24] A. Brodkorb, et al., INFOGEST static in vitro simulation of gastrointestinal food digestion, Nat. Protoc. 14 (4) (2019) 991–1014.
[25] S. Laiho, et al., Effect of whey protein phase volume on the tribology, rheology and sensory properties of fat-free stirred yoghurts, Food Hydrocoll. 67 (2017) 166–177.
[26] A. Sokolova, et al., Performance and characteristics of the BILBY time-of-flight small-angle neutron scattering instrument, J. Appl. Crystallogr. 52 (1) (2019) 1–12.
[27] C. Rehm, et al., Design and performance of the variable-wavelength Bonse–Hart ultra-small-angle neutron scattering diffractometer KOOKABURRA at ANSTO, J. Appl. Crystallogr. 51 (1) (2018) 1–8.
[28] O. Arnold, et al., Mantid—data analysis and visualization package for neutron scattering and μ SR experiments, Nucl. Inst. Methods Phys. Res. Sect. A: Accelerat. Spectromet. Detect. Assoc. Equip. 764 (2014) 156–166.
[29] L. Yu, et al., Multi-scale assembly of hydrogels formed by highly branched arabinoxylans from Plantago ovata seed mucilage studied by USANS/SANS and rheology, Carbohydr. Polym. 207 (2019) 333–342.
[30] B. Hammouda, A new Guinier–Porod model, J. Appl. Crystallogr. 43 (4) (2010) 716–719.
[31] M.Y. Lobanov, N. Bogatyreva, O. Galzitskaya, Radius of gyration as an indicator of protein structure compactness, Mol. Biol. 42 (4) (2008) 623–628.
[32] C.K. de Kruif, et al., Water holding capacity and swelling of casein hydrogels, Food Hydrocoll. 44 (2015) 372–379.